

Karst as a weathering skin phenomenon: Is there a simple, scale-independent model for karstification?

Stein-Erik Lauritzen
Department of Earth Science
Bergen University
Allegaten 41, N-5007 Bergen
stein.lauritzen@geo.uib.no

Abstract

Weathering reactions proceed from exposed surfaces into the rock mass and would be controlled by the rate of weathering, the rate of surface denudation and of inhibition factors. Combining these, it is possible to arrive at a relatively simple equation which describe the diffusion of a weathering, or karstification front into the rock mass. This effect has been tested on phenomena on a large variety of scales, from weathering varnish, phytokarst, epikarst, dolines and deep karst. These tests seem to confirm the Milanovich equation, describing exponential attenuation of karst voids with depth. This principle appear scale-independent over six orders of magnitude and is a solution of a simple, concentration-driven boundary-value problem.

Introduction

Karstification involves dissolution of the bedrock by means of water and acids that are transported into the rock mass. The products - mainly in homogeneous solution - are transported out of the karst, leaving a partly dissolved rock massif, which we call karst. Meteoric karst is a surface-related phenomenon; karstification penetrate from the (sometimes independently eroding) surface into the rock mass, Figure 1. Water flow through the karst is driven by gravity. It is obvious that these processes are complex, where reagents and solutes are distributed by turbulent dissipation and conveyed by highly unsteady flow, etc. so that molecular diffusion at first seems to be too much of a simplification to describe these processes in detail. However, classical diffusion is just a continuum description of a phenomenon that spreads similarly to a discrete random walk mechanism, and it is really only valid for a large number of individuals. These 'individuals' may be either molecules, packets of water, cavers or reindeer, and it is a matter of definition where we would distinguish between 'diffusion' and 'convection', etc. In this paper we will advocate that over longer timespans and space, some of the collective structures in karst may be explained to a large extent by diffusion-type mechanisms. This is supported by an accumulating amount of observations that the concentration of karst voids displays an exponential distribution with depth. These mechanisms also seem scale-independent over several orders of magnitude. The residuals between ground-truth data and the exponential model correspond to deviant zones that can be ascribed to rock structure or perhaps to 'levels'. It is interesting to note that such 'levels' are the targets of speleogenetic analysis.

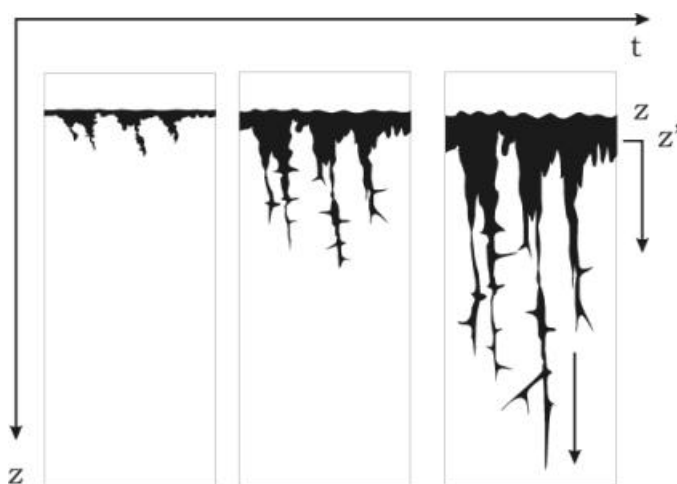


Figure 1.

Meteoric karstification penetrates from the surface into the rock mass. The land surface may be eroding independently, or as a result of total disintegration from the solution process.

Diffusion-type mechanisms.

Diffusion has been applied to models for small-scale chemical weathering, like the formation of weathering rinds (e.g. Hoke & Turcotte 2002). This can be applied to various phenomena like core-stone formation and obsidian hydration (Friedman & Long 1978). Such models lead to an exponential decay of weathering damage with depth from the attacked surface. It is tempting to test if such models are applicable to karst void concentration.

Simple diffusion of karst voids into a semi-infinite half-space may be described by the heat equation:

$$\frac{\partial q}{\partial t} = k \frac{\partial^2 q}{\partial z^2} \quad \begin{cases} q(z,0)=0 \\ q(0,t)=1 \\ q(\infty,t)=0 \end{cases} \quad (1)$$

where θ is the concentration of karst voids, or the amount of karst. κ is the diffusion constant (with dimension L^2/t), t time and z vertical distance. At the land surface, karstification is total ($\theta = 1$), at depth it approaches zero ($\theta(\infty) = 0$). Karstification also commences at a definite point in time ($\theta(z,0)=0$). The solution of this boundary value problem is valid for concentration-driven dissipation of various properties, like heat, particles, ions, etc. and is dealt with in many textbooks (Carslaw & Jaeger 1959, Crank 1975, Turcotte & Schubert 1982):

$$q(z,t) = q_0 \operatorname{Erfc}\left(\frac{z}{2\sqrt{\kappa t}}\right) \quad (2)$$

where Erfc is the complementary error function:

$$\operatorname{Erfc}(x) = 1 - \frac{2}{\sqrt{\pi}} \int_0^x e^{-x^2} dx \quad (3)$$

$\sqrt{\kappa t}$ is the characteristic diffusion distance, and consequently, $\gamma = z/2\sqrt{\kappa t}$ is a dimensionless ratio, or similarity variable. Series expansion of (3) and setting $\theta(z) = \theta_0/2$ in (2) yields $z_{1/2} \approx \sqrt{(\pi\kappa t)}/2 = 0.8862\sqrt{(\kappa t)}$, i.e. the time-dependent *half-depth of karstification*. If the process is controlled by diffusion alone, this depth will grow with the square root of time. Most of the change takes place near the surface along a boundary layer, which we may compare to either the epikarst or to the total explorable karst zone. Analogous to heat diffusion (Turcotte & Schubert 1982), the variable decays exponentially with depth so that an arbitrary definition of ‘thickness’ for the boundary layer must be made. The standard practise is to define the thickness of the boundary layer where $\theta(z) = 0.1 \cdot \theta_0$. Thus, from tables we find that $\gamma_{0.1} = \operatorname{Erfc}^{-1}(0.1) = 1.16$ and hence, $z_{0.1} = 2\gamma_{0.1}\sqrt{(\kappa t)} = 2.32\sqrt{(\kappa t)}$. Most previous analyses of karst voids, like dolines (White 1988), borholes (Milanovich 1981), caves and seismic velocities (Lauritzen 2001) used a simple exponential law:

$$q(z) = q_0 e^{-kz} \quad (4)$$

with half-depth $z_{1/2} = \ln 2/k$. If we assume that half-depth found by eqn (4) is the same physical distance as the one found by eqn (2), then the approximate link between the characteristic diffusion distance and the decay constant is:

$$k \approx \frac{\sqrt{\pi}}{2 \ln 2} \sqrt{\kappa t} \approx 1.279 \sqrt{\kappa t} \quad (5)$$

Eqn(2) describes chemical weathering penetration through a stationary surface ($z=0$), corresponding to the situation where karstification suddenly commences on a pristine rock surface, for instance after sudden uplift – a rather odd situation to be found in nature! From the scope of microscopic weathering, Hoke & Turcotte (2002) developed the diffusion concept further. After some initiation time (t_i), weathering will have progressed far enough to make the surface to fall apart, continuously changing the point of chemical attack at $z = 0$, resulting in a steady-state equilibrium between surface weathering and the progress of the weathering front. In the beginning, the weathering rind will develop with the square root of time, until $t = t_i$. After this, surface lowering and the progress of the weathering front is independent of time, i.e. the denudation rate is constant under constant hydrochemical conditions. We may regard surface disintegration as a direct analog to surface denudation in karst and the mass flux analogous to endokarst development or hydrochemical denudation. The coordinate system may be transformed by introducing a weathering velocity (v_D = surface denudation rate),

$$z = n_D(t - t_i) + z' \quad (6)$$

where t_i is the threshold or incubation time before surface denudation becomes apparent and z' the (moving) position of the land surface. Putting Eqn (6) into eqn (1), yields an expression for the steady state situation:

$$n_D \frac{dq}{dz'} = -k \frac{d^2 q}{dz'^2} \quad \begin{cases} q = q_0 & z' = 0 \\ q \rightarrow 0 & z \rightarrow \infty \end{cases} \quad (7)$$

with solution (Hoke & Turcotte op. cit.):

$$q = q_0 e^{-\left(\frac{n_D z'}{k}\right)} \quad \text{and} \quad n_D = \frac{1}{2} \sqrt{\frac{pk}{t_i}} \quad (8)$$

Eqn (8) then describes the depth-distribution of karst voids at steady state equilibrium in front of a moving top surface, where z' is the depth from the present-day land surface, v_D is the surface denudation rate, and κ the karst diffusion constant of eqn (1).

It is interesting to note that Eqn (8) is identical to eqn (4) with $k = v_D/\kappa$. In other words, the exponential decay model for karst concentration with depth chosen by Milanovic, White, and others is also a solution to an assumed dynamic diffusion process from a moving surface with boundary and initial value requirements of (7). The half-depth then becomes:

$$z_{1/2} = \ln 2 \frac{k}{n_D} \quad (10)$$

i.e. *the characteristic depth of karstification (here half-depth) increases with the diffusion constant, and decreases with surface denudation*. Equations (8) and (10) then describe an interesting relationship between surface denudation and endokarst development: if surface erosion rate is high, the characteristic depth of karstification decreases and may become zero. This is a characteristic feature of glaciated karst: independent glacial erosion may completely remove the epikarst and rejuvenate the whole process. From this, we may predict that the re-establishment of epikarst may progress with the square root of time until equilibrium is attained and surface denudation and epikarst progresses in pace at a constant rate.

Results and discussion

Data were collected from the original work of Milanovic (1981), from cross-sectional microphotographs of micro-phytokarst surfaces, from doline morphometry in Svartisen, Norway (Lauritzen 1996), from published doline morphometry (Troester et al 1984, White 1988), and from cave surveys and seismic tomography (Lauritzen 2001).

Estimates of the karst void concentration (θ) were collected from each data set and transformed to a dimensionless index (θ/θ_0), where θ_0 is the maximum density at the surface, i.e. eqn (8). Since the depth range of the studied objects span over six orders of magnitude (10 μ m to 300 m), depth was converted to dimensionless length $z/z_{1/2}$, where $z_{1/2}$ is the half-length determined from regression. In this way, depth becomes dimensionless in 'units' of half-depth. Results are listed in Table 1. All data are plotted in Figure 1. White (1988, p.35) suggests the use of $z_e = 1/k$ (eqn (4)) as the characteristic depth of dolines, which would scale to units of $1/e$ rather than half-depths. Although White's approach is more mathematically appealing, the concept of half- depth is easier to grasp for most people and is used here.

Weathering skin

Epoxy-cast and polished cross-sections of micro-phytokarstic weathering skins of various limestone surfaces were imaged under SEM and counted for void concentration as a function of depth. The observed concentration of colonization voids display an exponential decrease with depth from the surface with half-depths of 35- 40 μ m. Deviant concentrations were found along cracks and crystal interfaces. The establishment of micro-phytokarst in competition to intense corrosion in flowing water (Figure 2) depicts the effect of κ/v_D (eqn (10)). In flowing water, the denudation rate is greater than the diffusion rate of biological colonization ($\kappa < v_D$) so that no phytokarst skin develops, leaving the clean surface of corroded rock.

Epikarst and grikes

A data set of all ($n = 100$) grikes in the Graft Stripe karst of north Norway are well described with an exponential distribution with half-depth of 0.95 m (Lauritzen 1996). Similar half-depth (0.8 m) was found for the epikarst zone in arctic Norway, as analysed from a cross-hole seismic survey at a damsite (By et al. 1988). Please note that both epikarst sites are in formerly glaciated areas, where epikarst development might not have attained equilibrium with surface denudation, i.e. $t < t_i$ of eqn (6).

Dolines

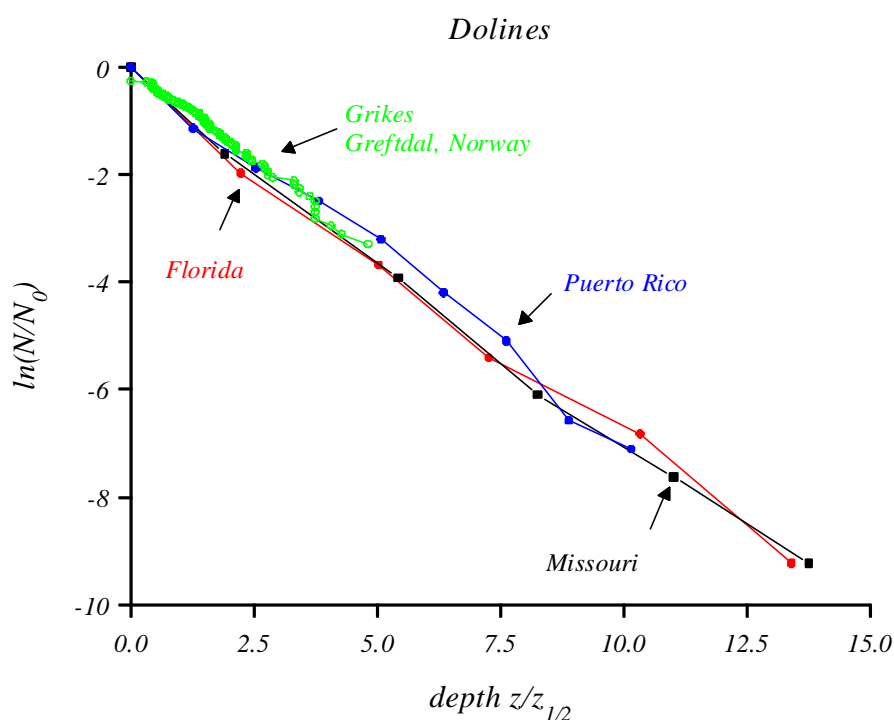
All doline data available were taken from the seminal work of Troester et al. (1984). Half-depths varies from epikarst dimension (Florida karst: 0.6 m) to deep tropical cockpits (8 m in Arecibo, Puerto Rico). Among the karst features investigated so far, grikes and dolines display the best fit to exponential distributions, Figure 3.

**Figure 2.**

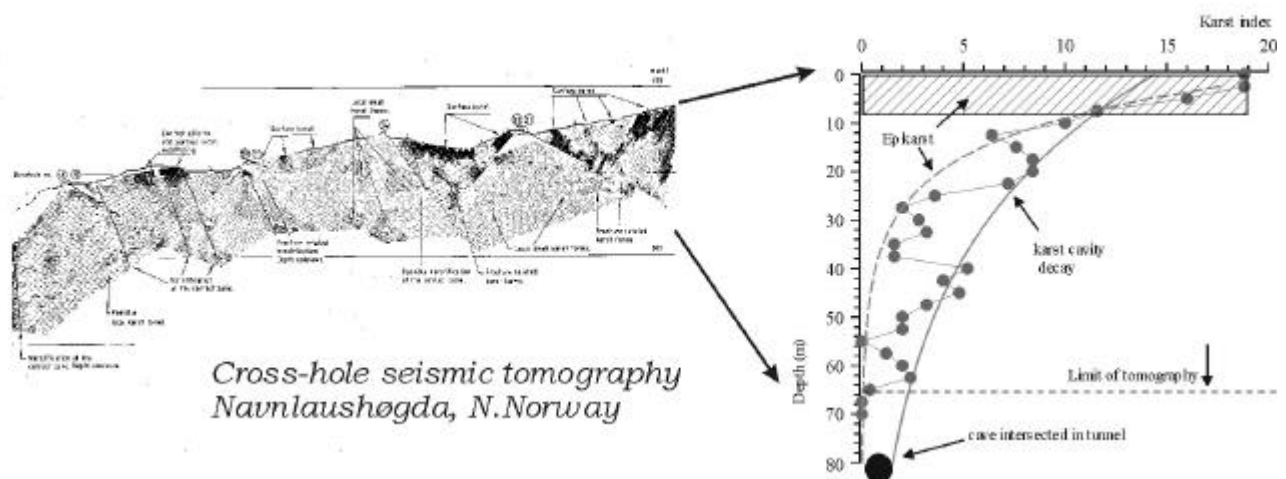
Competition between micro-phytokarst colonization and corrosion rate from running water, illustrating the importance of eqn (10). To the left, at the stream level, surface corrosion rate is greater than the microbial colonization rate, and a white, smooth marble surface results. The stream corrosion rate (n_D) is about 0.3 mm/yr. To the right, where a micro-phytokarst skin has developed, the denudation rate ($n_D = 0.025$ mm/yr) is only due to atmospheric precipitation.

Endokarst

Few reliable cave data exists, but Lauritzen (2001) argued that well- explored and surveyed cave systems in vertical stripe karsts may provide a relatively true picture of the density of human-sized cave passages. The Salthølene system display a half-depth of 65 m; this is very close to the half-depth (60 m) of the original distribution function of Milanovic (1981), based on 146 borehole logs in the Dinaric karst. The endokarst component of the seismic survey of By et al. (1988), as analysed by Lauritzen (2001) display a half-depth of only 25 m. This lower value may perhaps reflect a disequilibrium situation due to glacial erosion.

**Figure 3.**

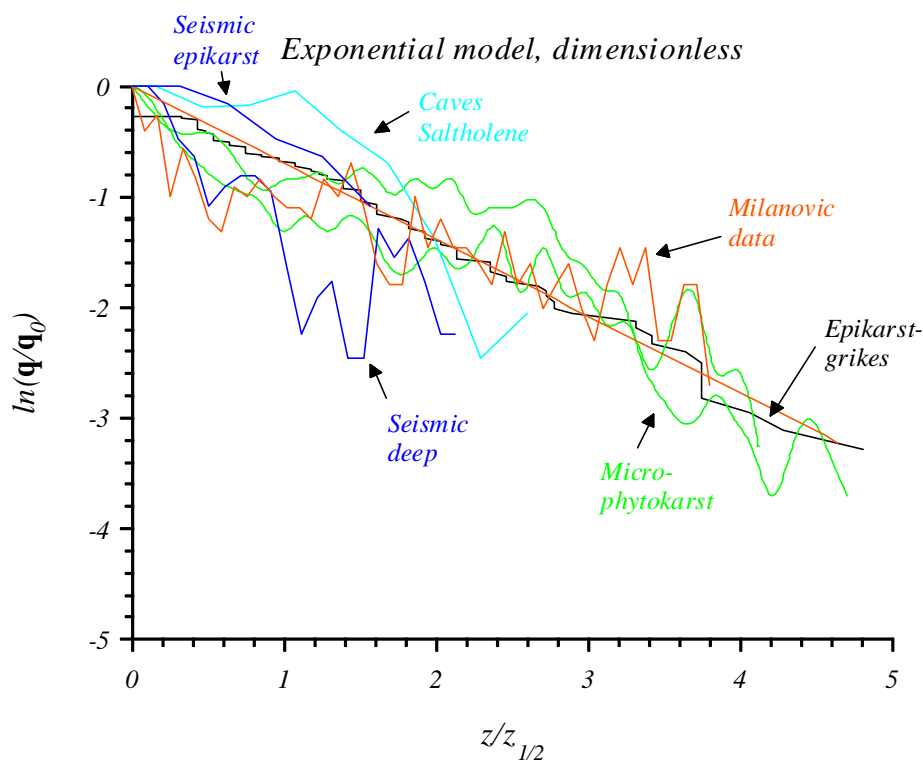
Frequency distribution of dolines and epikarst grikes from north Norway as a function of dimensionless depth. Data from Troester et al (1984) and Lauritzen (1996).

**Figure 4**

Left: Seismic tomography at a damsite in north Norway (By et al. 1988). Right: Depth-frequency of low-velocity zones ('karst'), two exponential decay functions are used, one for the epikarst zone and one for the deeper karstification (Lauritzen 2001).

Deviations from the smooth distribution

The residuals, or deviation from these smooth distributions contain the most interesting information. Deviations occur where the density of karst voids are greater or less than predicted from the model. Since karst density is projected vertically from the surface (along the z -axis), these deviations would correspond to 'levels'. Most likely, these features represent geological structure and perhaps hydrological levels. These features are truly the most interesting phenomena in karst as they would represent the hydrological anomalies that distinguish karst aquifers from all other aquifers. In fact, these deviant features may also be the most significant and interesting in the context of speleogenetic analysis. More speculative, we may perhaps interpret deviations as a result of a variable forcing function, e.g. long-term climatic change that would propagate a 'wave' of enhanced or retarded karstification through the rock mass. These ideas remain to be investigated.

**Figure 5.**

All data, except dolines, plotted together. The data sets cover six orders of magnitude and demonstrate that the exponential approximation is valid over this range.

Conclusions.

Karst features over a scale range of six orders of magnitude can be adequately described by exponentially decaying depth distributions. Exponential depth distribution is a solution of the diffusion equation operating from an independently eroding or denuding surface. In this context, 'diffusion' means a process that is driven by concentration gradients. We may therefore suggest that karst features on the collective scale may be described as a result of this kind of process, although the residuals may perhaps represent the features of greatest interest.

Table 1.
Half-depth of some exponentially-distributed karst features

Feature	Object	$Z_{1/2}$ (m)	Regression fit (r^2)
Weathering skin	Micro-Phytokarst 1 ¹	$3.5 \cdot 10^{-5}$	0.83
	Micro-Phytokarst 2 ¹	$4.0 \cdot 10^{-5}$	0.76
Epikarst	Grikes, Greftdal ²	0.95	0.99
	Cross-Hole seismic ³	0.79	0.92
Dolines	Florida ⁴	0.58	0.99
	Missouri ⁴	2.2	0.99
	Puerto Rico ⁴	7.9	0.99
Endokarst	Saltholene caves ³	65	0.79
	Cross-hole seismic ³	25	0.98
	Bore-holes Dinaric karst ⁵	59	0.81

¹ Lauritzen (2005) unpublished; ² Lauritzen (1996); ³ Lauritzen (2001); ⁴ Troester et al. (2004); ⁵ Milanovic (1981);

References

- By, T.L. ; Lund, C. & Korhonen, R. 1988: Karst cavity detection by means of seismic tomography to help assess possible dam site in karst terrain. Pp. 25-31 in: Romana (Ed) *Rock mechanics and Power Plants*. Balkema, Rotterdam.
- Carlslaw, H.S. & Jaeger, J.C. 1959: *Conduction of Heat in Solids*. 2nd ed. Clarendon Press. Oxford. 510 pp.
- Crank, J. 1975: *The Mathematics of Diffusion*. Clarendon Press. Oxford. 414 pp.
- Friedman, I. & Long, W. 1978: Hydration of obsidian. *Science* **191**, pp. 347- 352.
- Hoke, G.D. & Turcotte, D. L. 2002: Weathering and damage. *Journal of geophysical research*, **107**:2210.
- Lauritzen, S.E. 1996: *Karst landforms and caves of Nordland, North Norway. Guide for Excursion 2, Climate Change: the Karst Record, august 5th – 16th 1996*. Department of Earth Science, Bergen University. 160 pp.
- Lauritzen, S.E. 2001: Marble stripe karst of the Scandinavian Caledonides: and end-member in the contact karst spectrum. *Acta Carsologica* **30** (2) 47-79.
- Milanovic, P. 1981: *Karst Hydrogeology*. Water-resources Publications. Colorado. 434 pp.
- Troester, J.W., White, E.L. & White W.B. 1984: A comparison of sinkhole depth frequency distributions in temperate and tropic karst regions. *Proceedings of the First Multidisciplinary Conference on sinkholes, Orlando Florida. (ED. Beck, BF) Balkema, Totterdam*
- Turcotte, D.L. & Schubert, G. 1982: *Geodynamics. Application of Continuum Physics to geological Problems*. John Wiley & Sons. New York. 450 pp.
- White, W.B. 1988: *Geomorphology and Hydrology of Karst Terrains*. Oxford University Press. New York. 464 pp.